LBL-30464

Lawrence Berkeley Laboratory
UNIVERSITY OF CALIFORNIA

Accelerator & Fusion
Research Division

Presented at the Fourth International Conference on Synchrotron Radiation Instrumentation, Chester, United Kingdom, July 14–19, 1991, and to be published in the Proceedings

Determining Surface Profile from Sequential Interference Patterns from a Long Trace Profiler

S.C. Irick

July 1991

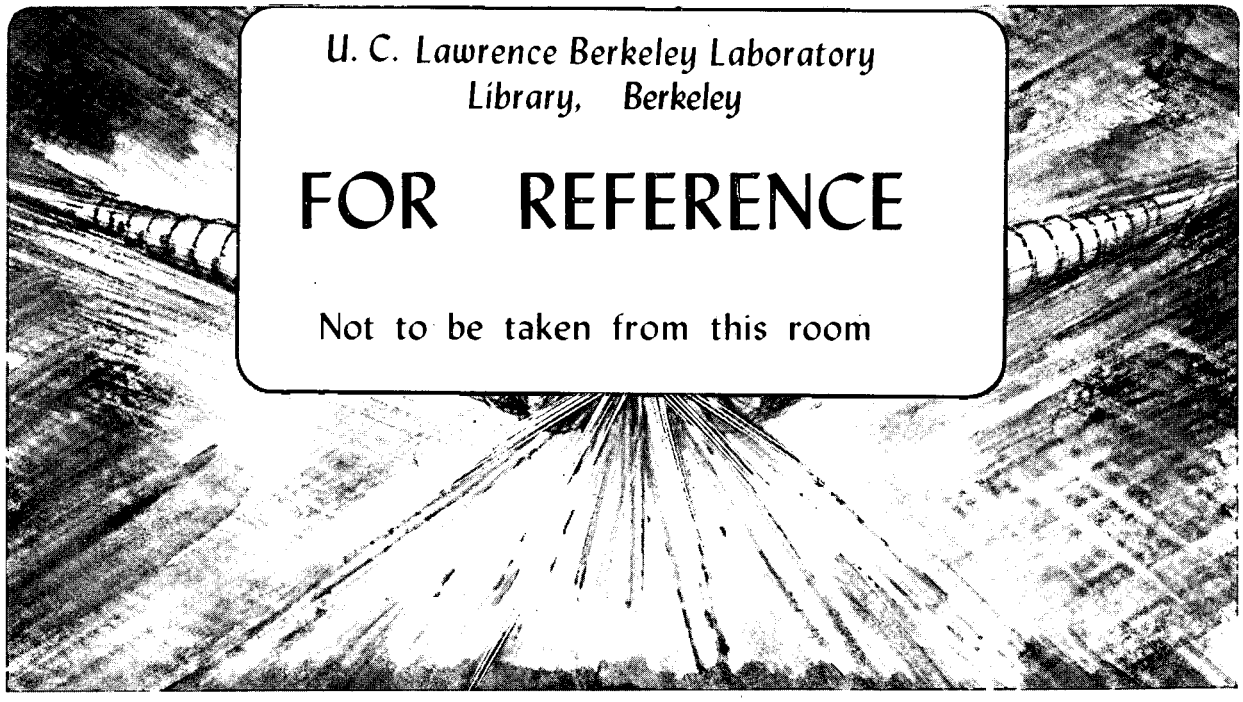

Prepared for the U.S. Department of Energy under Contract Number DE-AC03-76SF00098

DISCLAIMER

DISCLAIMER

LBL-30464

Determining Surface Profile from Sequential Interference Patterns from a Long Trace Profiler*

S. C. Irick

Advanced Light Source
Accelerator and Fusion Research Division
Lawrence Berkeley Laboratory
University of California
Berkeley, CA 94720

July 1991

Paper Presented at the Synchrotron Radiation Instrumentation Conference, Chester, England, July 14–19, 1991

*This work was supported by the Director, Office of Energy Research, Office of Basic Energy Sciences, Materials Sciences Division of the U.S. Department of Energy, under Contract No. DE-AC03-76SF00098

Determining Surface Profile from Sequential Interference Patterns from a Long Trace Profiler

S. C. Irick

Accelerator and Fusion Research Division
Lawrence Berkeley Laboratory
University of California
Berkeley, CA 94720 USA

Abstract

The Long Trace Profiler (Takacs et al.) is a slope-measuring instrument which was introduced several years ago. Development of this instrument continues at Lawrence Berkeley Laboratory in improving both hardware design and software algorithms for turning the raw interference data (a sequence of intensity patterns) into properly interpreted representations of surface slope and height. This report presents a mathematical model of the interference pattern and methods of extracting the slope and height profile from such patterns.

Introduction

The Long Trace Profiler is an instrument which measures slope in the long (meridional) dimension of a long optical surface. Such surfaces are typically mirrors or diffraction gratings that are used in X-ray equipment, and therefore have a large ratio of length to width. These mirrors and gratings are used in configurations where the light strikes the surface at near grazing incidence. In this kind of optical system, variations from an optimal surface in the sagittal direction affect the performance relatively little, while meridional variations almost completely determine performance of the optic. Thus, an instrument is needed that will characterize the surface in the long dimension (along the x axis) and that will give an accurate profile of the surface with spatial periods as long as the optic.

The Long Trace Profiler (LTP) described here was developed by Peter Takacs[1,2] and uses the principle of the pencil beam interferometer described by Von Bieren[3,4]. In principle, two beams from the same laser are reflected from a surface under test (SUT) and combined to form an interference pattern. The relative phase between the beams after reflection from the SUT is determined by the shape and position of the intensity pattern. In turn, the relative slope of the SUT at that point is determined by this relative phase.

To understand how relative slope is obtained from relative phase, consider a pair of light beams which, before hitting a mirror, are in phase (ie, $\phi_i = 0$). After reflection from a mirror, the relative phase ϕ of one beam with respect to the other along the intrument's optic axis $\mathbf{k_i}$ will depend on the angle θ of the mirror's normal $\mathbf{n}$ with respect to the beams' propagation direction, also $\mathbf{k_i}$; see Figure 1. The slope is

$$m(x) \;=\; \tan\theta \;=\; \frac{\Delta y}{\Delta x} \;=\; \frac{(\phi/2\pi)(\lambda/2)}{\Delta x} \;=\; \frac{\lambda\,\phi}{4\pi\Delta x}, \tag{1}$$

where λ is the wavelength of the beams.

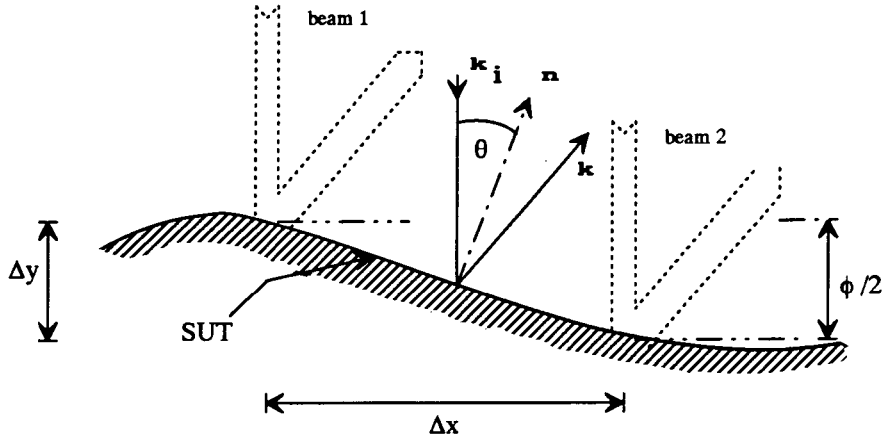

Figure 1. Relationship between slope of SUT and phase difference.

Of course, the incident beams aren't required to be in phase; we are only interested in relative slope along the surface. Therefore, we look for the change in phase between the two beams from one place x on the SUT to the next place $x + \Delta x$.

Determining Phase Difference between the Beams

When two beams of light from the same laser are brought together, the waves that describe the beams combine according to the superposition principle and form standing waves in the common volume of the two beams. After reflection from the SUT, each of the two beams is at first collimated and is approximately parallel to the optic axis of a Fourier transform (FT) lens. The FT lens causes the two beams to come together in the FT lens back focal plane (bfp), as in Figure 2. The phase difference between the two beams shows up in the standing wave pattern as the placement of the standing wave maxima, or of the peaks in the intensity pattern there.

The phenomenon here is similar to that of Young's double slit experiment[5], where two coherent wavefronts in the front focal plane (ffp) are brought together to form a Fraunhofer diffraction pattern which is modulated by a sinusoidal interference pattern. If the optical path of one of the wavefronts is increased with respect to the other wavefront, the phase of the sinusoidal interference pattern will change, causing the pattern to shift to the right or left.

Since each beam is from a laser, the amplitude distribution perpendicular to each beam axis is Gaussian. Therefore, the intensity distribution along the v axis will be a Gaussian form modulated by a sinusoid.

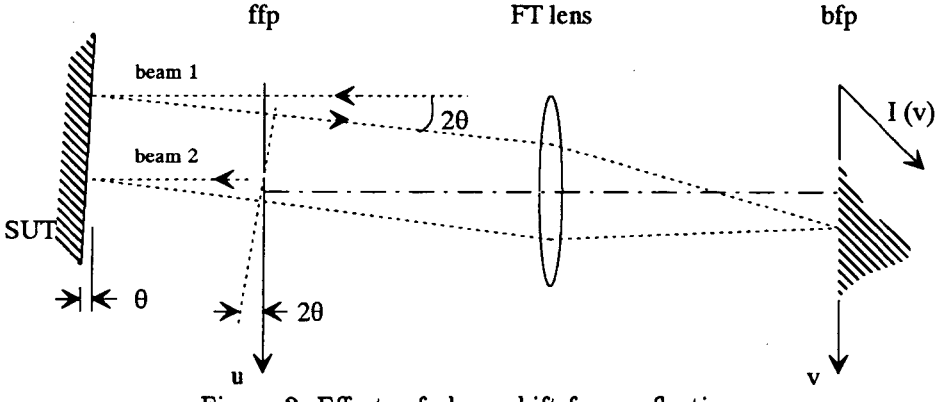

Figure 2. Effects of phase shift from reflection.

Also notice that reflection from the SUT at an angle $\theta \neq 0$ causes the phasefront of each beam to be

tilted with respect to the u axis (ffp). The tilt of the phasefront defines the propagation direction of the beams, and determines the amount of lateral shift of the whole interference pattern along the v axis (bfp). The value of relative phase ϕ along the u axis of either beam can be found from the tilt of the phasefront, and is

$$\phi(u) \quad = \quad \frac{2\pi}{\lambda} u \tan(2\theta) \quad \simeq \quad \frac{4\pi}{\lambda} u \tan(\theta) \quad = \quad \frac{4\pi}{\lambda} m(x) u. \tag{2}$$

For a fixed $u = \Delta x$, $\phi(u) = \phi$ and Equation (2) is equivalent to Equation (1).

Quantifying the Intensity Pattern at the Detector Array

In the LTP, a detector array is placed in the bfp so that the intensity pattern of the standing waves may be observed. In general, the complex amplitude of the standing waves in the bfp will be the Fourier transform of the complex amplitude in the ffp, assuming the FT lens is diffraction limited and the amplitude pattern at the lens is within the lens' aperture.

Occasionally the transform of a function $f(x)$ will be denoted by $\mathcal{F}\{f(x)\}$. Usually, however, Bracewell's[6] notation will be used to show the relationship between a function and its transform:

$$f(x) \quad \supset \quad \mathcal{F}\{f(x)\}.$$

The cross sectional amplitude distribution of a laser beam may be described ideally by a Gaussian function $\exp[-u^2/R^2]$, where R is the "$1/e^2$" radius of the laser beam. The amplitude distribution of both beams at the ffp is shown in Figure 3 (a). Notice that Figure 3 (a) is the convolution of one Gaussian with a pair of impulses which are separated equally about $u = 0$ by d. The convolution theorem states that the convolution between two functions $f(t)$ and $g(t)$ has a Fourier transform

$$f(t) \otimes g(t) \quad \supset \quad \mathcal{F}\{f(t)\} \times \mathcal{F}\{g(t)\}, \tag{3}$$

where "$\otimes$" is the convolution operator.

Therefore, the amplitude in the bfp is the product of a cosine (transform of an impulse pair) and a Gaussian (transform of a Gaussian). These functions and their transforms are (see Bracewell[7]):

$$\exp[-\pi u^2] \quad \supset \quad \exp[-\pi v^2] \qquad \text{(Gaussian amplitude)}; \tag{4}$$

$$\tfrac{1}{2}\delta(u + \tfrac{1}{2}) \quad + \quad \tfrac{1}{2}\delta(u - \tfrac{1}{2}) \quad \supset \quad \cos(\pi v) \qquad \text{(impulse pair)}. \tag{5}$$

Using the similarity theorem for Fourier transforms, we now include the parameters at the ffp:

$$\exp[-a\pi u^2] \quad \supset \quad \frac{1}{|a|} \exp[-\frac{\pi}{a} v^2]. \tag{6}$$

Let $a = \frac{1}{\pi R^2}$.

$$A_G(u) \quad = \quad \exp[-u^2/R^2] \quad \supset \quad \pi R^2 \exp[-\pi^2 R^2 v^2]. \tag{7}$$

This describes the Gaussian amplitude component.

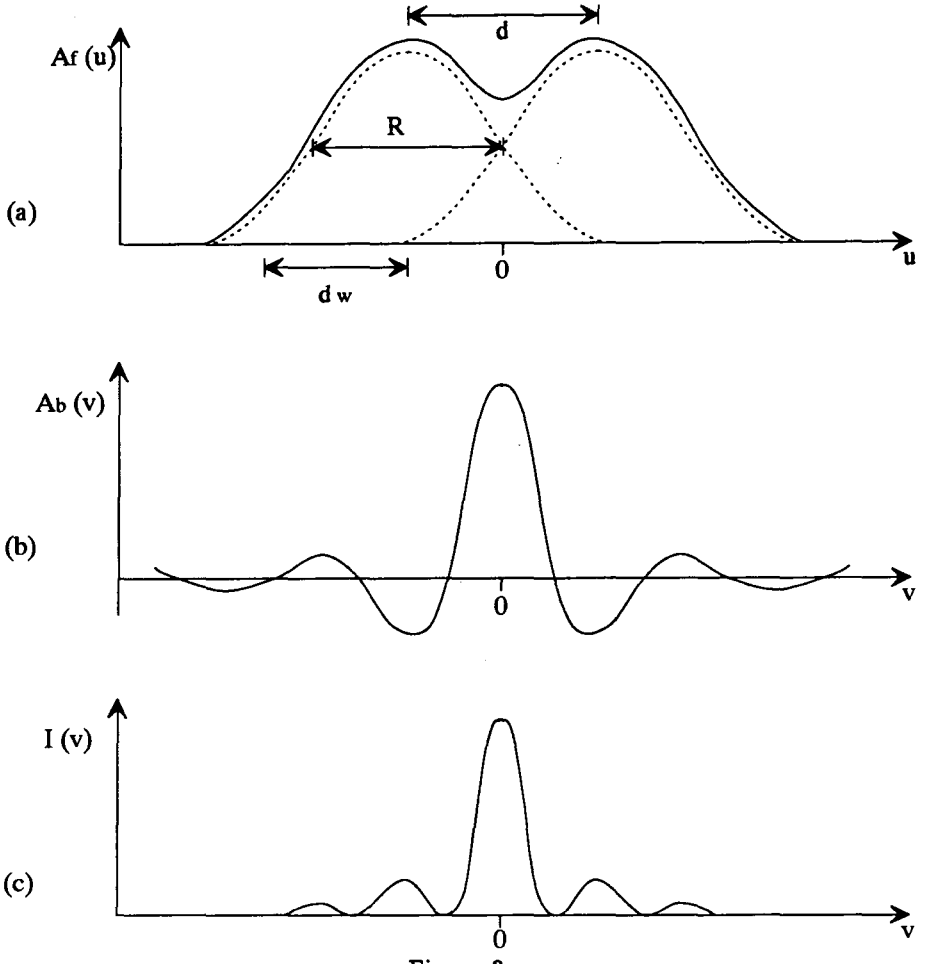

Figure 3.

(a) Amplitude part of the complex amplitude in the ffp. (b) Amplitude part of the complex amplitude in the bfp. (c) Intensity pattern in the bfp.

We do likewise for the impulse pair component. If $\mathcal{F}\{f(t)\} = F(s)$ and $f(t) = \cos(a\pi t)$, then $F(s) = \frac{1}{2}\delta(s + a/2) + \frac{1}{2}\delta(s - a/2)$. In Equation (5) the spacing between impulses is 1, so that the impulses (delta functions) are located at $u = -\frac{1}{2}$ and $u = +\frac{1}{2}$ respectively. When the spacing is d,

$$A_\delta(u) \quad = \quad \tfrac{1}{2}\delta(u + d/2) \quad + \quad \tfrac{1}{2}\delta(u - d/2) \quad \supset \quad \cos(\pi dv). \tag{8}$$

Now we combine Equations (7) and (8) using Equation (3):

$$A_G(u) \otimes A_\delta(u) \quad \supset \quad \pi R^2 \exp[\pi^2 R^2 v^2] \quad \times \quad \cos(\pi dv). \tag{9}$$

The left side of Equation (9) describes the amplitude $A_f(u)$ in the ffp, while the right side describes the amplitude $A_b(v)$ in the bfp. In order to take into account the phase shift (as shown in Figure 2), $A_f(u)$ must be multiplied by a phase shift term:

$$A_f(u) \quad = \quad [A_G(u) \otimes A_\delta(u)] \quad \times \quad \exp[-i\phi(u)]. \tag{10}$$

Equation (2) is substituted to express this in terms of slope:

$$A_f(u) \quad = \quad [A_G(u) \otimes A_\delta(u)] \quad \times \quad \exp[-i2\pi(2m(x)/\lambda)u]. \tag{11}$$

According to the shift theorem for Fourier transforms,

$$\exp[-i2\pi as]\ F(s) \quad \supset \quad f(t-a). \tag{12}$$

This allows us to express $A_b(v)$ in terms of a lateral shift of the interference pattern. Using the concept of Equation (12) to combine Equations (9) and (11) gives:

$$\begin{aligned}[A_G(u) \otimes A_\delta(u)] \ \times \ \exp[-i2\pi(2m(x)/\lambda)u] \\ \supset \quad \pi R^2 \exp[-\pi^2 R^2 (v - 2m(x)/\lambda)^2] \ \times \ \cos(\pi d(v - 2m(x)/\lambda)).\end{aligned} \tag{13}$$

At this point the constant factor πR^2 may be removed:

$$A_b(v) \quad = \quad \exp[-\pi^2 R^2 (v - 2m(x)/\lambda)^2] \ \times \ \cos(\pi d(v - 2m(x)/\lambda)). \tag{14}$$

The amplitude function $A_b(v)$ in the bfp is purely real, because the amplitude function which describes the convolution of the Gaussian with the impulse pair is Hermitian. In other words, we need not be concerned with the phase values in the intensity pattern. But when the beams come in at the ffp not centered with respect to $u = 0$, the amplitude will no longer be Hermitian; even so, the intensity pattern in the bfp will not change if the FT lens is of good quality (diffraction limited). $A_b(v)$ is shown in Figure 3 (b).

Of course the detector array only sees intensity, which is the amplitude in the back focal plane times its complex conjugate (see Figure 3 (c)):

$$\begin{aligned} I(v) &= A_b(v) \ \times \ A_b^*(v) \\ &= \{\exp[-\pi^2 R^2 (v - 2m(x)/\lambda)^2] \ \times \ \cos(\pi d(v - 2m(x)/\lambda))\}^2 \\ &= \exp[-2\pi^2 R^2 (v - 2m(x)/\lambda)^2] \ \times \ \cos^2(\pi d(v - 2m(x)/\lambda)) \\ &= \exp[-2\pi^2 R^2 (v - 2m(x)/\lambda)^2] \ \times \ [\tfrac{1}{2} + \tfrac{\mu}{2} \cos(2\pi d(v - 2m(x)/\lambda))]. \end{aligned} \tag{15}$$

The factor μ is the modulation factor and is included to represent a number of phenomena which could reduce the visibility of the cosine component. Examples of such phenomena are finite coherence length of the laser with unequal beam path length (small effect in the LTP) and unequal intensity of one beam with respect to the other. If these phenomena are not present, then $\mu = 1$.

Suppose that a change in $m(x)$ causes the quantity $2m(x)/\lambda$ to change by some amount on the v axis. Then the part of the intensity pattern represented by the factor $\exp[-2\pi^2 R^2 t^2]$ will move the same absolute distance on the v axis as the part represented by the factor $\cos(2\pi dt)$. I.e., the cosine component and the Gaussian component will move together along the v axis as the slope of the SUT changes.

Extracting Phase from the Intensity Pattern

So far we have a model of the intensity pattern at the detector array (Equation 15), and we wish to determine $m(x)$. In this report we consider two methods for determining the relative slope at any point on the SUT.

Takacs and Feng[2] determine the phase, and hence the relative slope, by fixing attention on one point of the cosine component and assuming that phase is proportional to this point's position on the detector array (see Figure 4). As the slope of the SUT changes, the position of one point on the cosine moves. This point is taken to be a local minimum of the cosine function and is found by fitting a parabola to a few points in less than one half cycle of the cosine.

One normally thinks of phase as a real number limited to values between $-\pi$ and π (maybe between 0 and 2π). In this case, slopes would be limited to values between $-\lambda/(4d)$ and $+\lambda/(4d)$ (or between 0 and $\lambda/(2d)$). Takacs solved this problem with the concept of a "pixel function" $P(x)$. The pixel function relates the position of the minimum point on the cosine half cycle directly to slope, thus giving a total (as opposed to modulo 2π) phase value all along the detector array. From Figure 4 the pixel function would be the set of numbers $P(x) = \{\ldots, v_i, v_{i+1}, \ldots\}$. The slope is then proportional to the pixel function.

$$m(x) \quad = \quad K_1 \; P(x), \tag{16}$$

where $K_1 = L/(2Nf)$. L is the detector array length, N is the number of elements in the array, and f is the FT lens focal length.

Takacs knew which cycle of the cosine this minimum point should be, because he chose the spacing d in the ffp to be approximately the width of one beam, which makes the modulating envelope in the bfp (Gaussian component) contain less than two cosine cycles. Another reason for choosing the spacing d to be the width (d_w in Figure 3) of one beam is that optimum sampling criteria are met.[8]

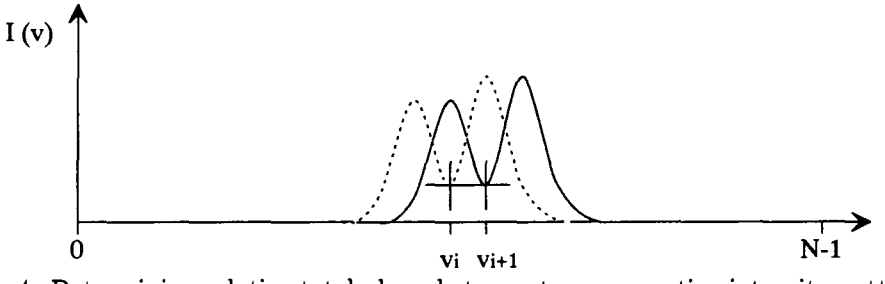

Figure 4. Determining relative total phase between two consecutive intensity patterns.

Now let us consider another method of determining $m(x)$. If the intensity pattern was formed by taking the Fourier transform of function $A_f(u)$ representing the amplitude in the ffp, then this original function can be obtained by taking the inverse Fourier transform of $A_b(v)$. Recall that the amplitude $A_b(v)$ can be taken as purely real, because $A_f(u)$ is Hermitian. This assures that the intensity $I(v)$ carries all the information necessary to reconstruct the amplitude in the ffp; thus $m(x)$ is determined precisely.

The inverse Fourier transform (or just "transform", since the only difference is a reversal of the abscisssa, or w axis) of I(v) will be similar to $A_f(u)$, but it will contain an extra impulse component at the center (at $w = 0$). This is because we are taking the transform of $\cos^2(t)$, which is the transform of $\cos(2t)$ plus a "dc" term. The transform of the cosine component with dc is shown in Figure 5 (a). The transform of the Gaussian envelope is shown in Figure 5 (b). The transform of the product of the cosine (with dc) and the Gaussian is a convolution of the transform of the cosine (with dc) with the transform of the Gaussian, and is shown in Figure 5 (c).

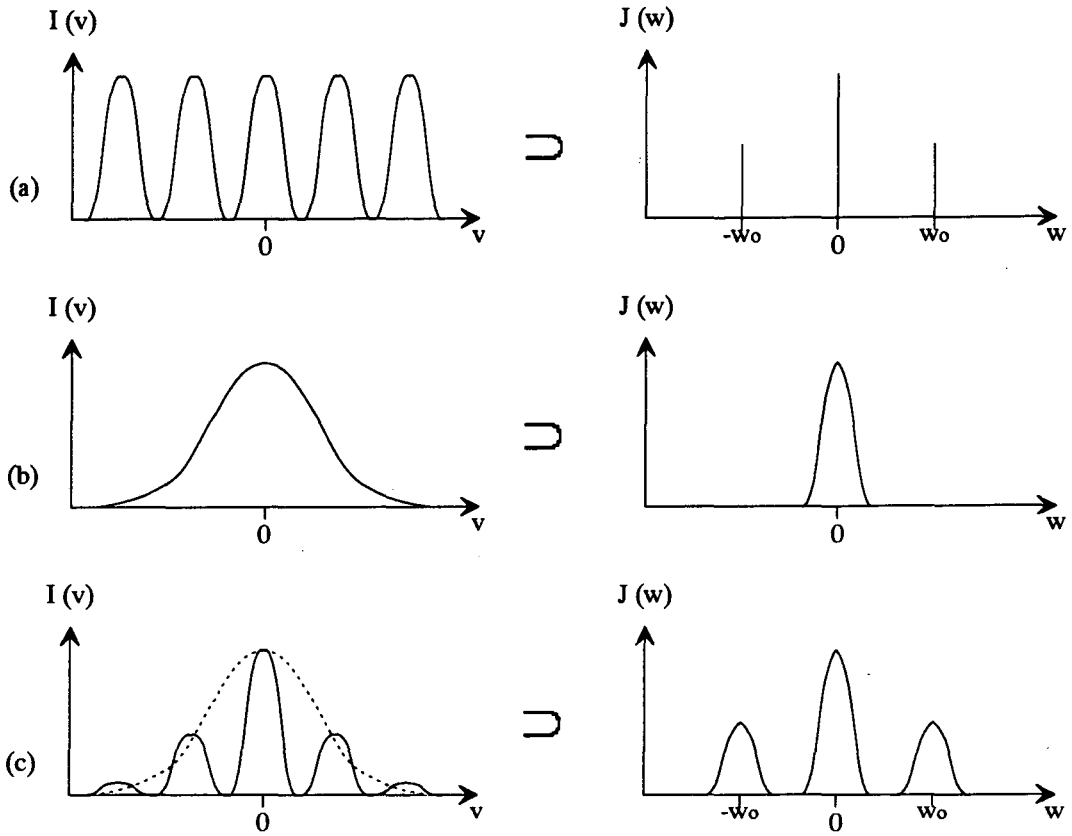

Figure 5. Amplitude components of the transform of the intensity pattern.

The phase difference ϕ between impulses in $A_f(u)$ will be equal to the phase at $-w_0$ (or equal to the negative phase at $+w_0$) in $J(w)$ (the transform of I(v)). It would seem that determining ϕ is as simple as finding the phase value at $w = -w_0$, which is at the only peak to the left of $w = 0$ in Figure 5 (c). However, the phase value anywhere is modulo 2π, not the total phase. The solution is to look at the phase change for the entire pattern in the same way that we would look at the tilt in the phase as shown in Figure 2.

$$\phi(w) \quad = \quad K_2 \frac{4\pi}{\lambda} m(x) w \tag{17}$$

K_2 is a constant that relates the magnification between the axes u and w. $K_2 dw = \lambda f / L$. The phase values for $J(w)$ will change in the vicinity of $\pm w$ proportionally to the amount that the sinusoidal pattern in $I(v)$ is shifted on the v axis. The slope is then obtained by differentiating Equation 17 with respect to w:

$$m(x) \quad = \quad \frac{\lambda}{4\pi K_2} \frac{d\phi}{dw}. \tag{18}$$

Comparison of the Two Slope Calculation Methods

Calculation of accurate slope values depends on how accurately K_1 or K_2 is determined. Determinations of K_1 and K_2 are similar. Probably the most difficult quantity to accurately determine is f. However, this problem can be dealt with by calibrating the LTP with a known slope at the SUT.

Measurement of relative slopes can be made on a known SUT for comparing the two methods. However, the only test surface whose slopes are well known by an independent measurement is a flat. Therefore, measurement of a flat was chosen to compare the two methods. Also, to eliminate any deviation from flatness, the LTP was made to measure the same position on the SUT. This in-place measurement method essentially measures the noise of the LTP and calculation method, but does not include noise caused by a normal optical carriage movement. (The optical carriage is the interferometer probe that moves along the SUT.) Thus, an in-place measurement would give the most unbiased assessment of the slope calculation method.

Figures 6 and 7 show a typical in-place measurement of 100 points on a smooth flat. Both measurements give similar results. In this case the quality of the interference patterns was very good; they looked very much like the pattern in Figure 4. A comparison of the two methods in this case is inconclusive in determining that one method is overwhelmingly better. Both methods show similar structure, the most important being a gradual decrease in the slope due to either thermal dimensional changes or mechanical stress relief in the mounting of the optic.

When the patterns become noisy with high frequency components the Fourier transform method (second method) is the better method to use, because choosing phase values only in the vicinity of $\pm w$ filters out the noise in the other frequencies. On the other hand, if the beam spacing d tends to change during a measurement, the curve fitting method is better to use. This is because when the beam spacing changes, the cosine component stretches about the intensity pattern's centroid. If the minimum value (v_i in Figure 4) of the cosine component is close to the intensity pattern centroid, then a change in d will affect the calculated slope very little.

Figure 6. Slope calculated by curve fitting method.

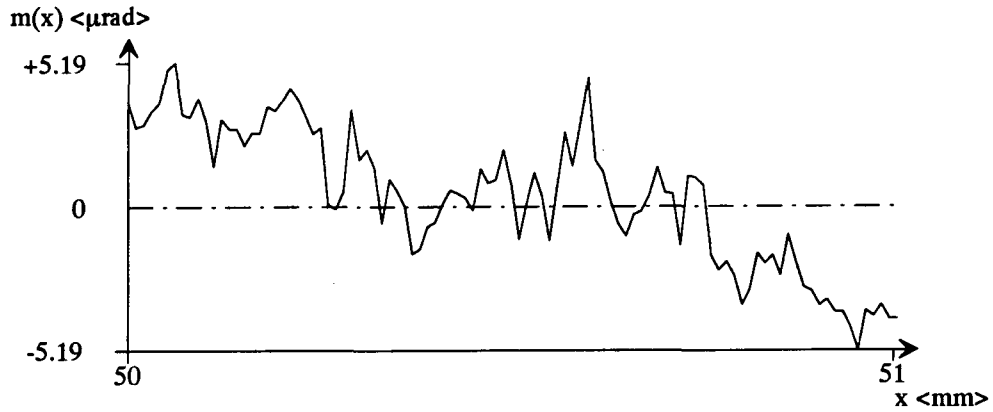

Figure 7. Slope calculated by Fourier transform method.

Another drawback of the curve fitting method is that the initial phase difference between the beams must be such that the interference pattern is a smooth, symmetric double peak. Any deviation from this will improve chances for the curve fit to be made on an undesired part of the pattern, and thus give erratic slope values. However, the speed of fitting a curve is so much greater than taking a Fourier transform that the curve fitting method is very attractive if the interference pattern has a good shape.

Determining the Height Profile

Converting the slope function $m(x)$ to a height profile is done by simply integrating the slope function over the abscissa x. Perhaps the simplest and fastest method is the trapezoidal integration method. Other methods may render a more realistic height profile, and therefore would be more accurate. However, since a Fourier transform function would be used elsewhere in the computer program, it is fairly simple to use the transform to convert slope to height. The height function is

$$h(x) \quad = \quad \int_{x=scanstart}^{x=scanstop} m(x)dx \quad = \quad \mathcal{F}^{-1}\{\mathcal{F}\{m(x)\}/(i2\pi x')\}. \tag{19}$$

x' is the transform domain axis which is the same as x, and $\mathcal{F}^{-1}$ is the inverse FT operator.

Weaver[9] discusses several of these integration methods and compares their expected errors.

Conclusion

Two methods for calculating the slope of a surface from interferometric patterns have been presented. Results of the two calculation methods have been compared using a simple in-place measurement of a flat surface. Both measurement methods give similar results, but each is affected differently by certain characteristics that make up noise in the data. Depending on the severity of one characteristic of the noise (e.g., changing beam separation or high frequency coherence noise), one calculation method will give better results than the other.

Acknowledgements

This work was supported by the U. S. Department of Energy under Contract No. DE-AC03-76SF00098. Thanks to Wayne McKinney for encouraging development of optimum slope calculation algorithms; to Brian Kincaid for discussions on Fourier transform techniques; and to Akiko and Julia for agreeing to move to California.

References

1. P. Z. Takacs and S. Qian, **United States Patent** No. 4884697 (5 Dec., 1989).

2. P. Z. Takacs, S. K. Feng, E. L. Church, S. Qian andW. Liu, "Long trace profile measurements on cylindrical ashperes," Proc. SPIE, **966**, 354-364 (1988).

3. K. von Bieren, "Pencil beam interferometer for aspherical optical surfaces," in **Laser Diagnostics**, Proc. SPIE, **343**, 101-108 (1982).

4. K. von Bieren, "Interferometry of wavefronts reflected off conical surfaces," Appl. Opt., **22**, 2109 (1983).

5. F. A. Jenkins and H. E. White, *Fundamentals of Optics*, McGraw-Hill, New York (1957).

6. R. N. Bracewell, *The Fourier Transform and Its Applications*, Second Edition, McGraw-Hill, New York (1978).

7. Bracewell, Op. Cit., chapter 6, p. 101.

8. E. L. Church, "Design notes for a profiling instrument," (personal communication) (31 Dec, 1985).

9. H. J. Weaver, *Applications of Discrete and Continuous Fourier Analysis*, John Wiley and Sons, New York (1983).

LAWRENCE BERKELEY LABORATORY
UNIVERSITY OF CALIFORNIA
INFORMATION RESOURCES DEPARTMENT
BERKELEY, CALIFORNIA 94720